DESIGNING ASIAN-SIZED HAND MODEL FOR SAR DETERMINATION AT GSM900/1800: SIMULATION PART

S. H. Ronald[1, *], M. F. A. Malek[1], S. I. S. Hassan[1], C. E. Meng[2], M. H. Mat[1], M. S. Zulkefli[1], and S. F. Maharimi[3]

[1]School of Electrical System Engineering, University Malaysia Perlis, Perlis 01000, Malaysia

[2]School of Mechatronic Engineering, University Malaysia Perlis, Perlis 01000, Malaysia

[3]School of Computer and Communication Engineering, University Malaysia Perlis, Perlis 01000, Malaysia

Abstract—A simple geometrical Asian-hand model with human tissue properties posed at two common talk-mode positions is proposed for comparative study. The newly designed hand is formed by measuring an adult female hand at open-hand position before being posed into the presented styles. Four human hand tissues are included: skin, bone, muscle, and tendon, and also three homogeneous sets of hands using specific anthropomorphic mannequin (SAM) hand phantom dielectric properties. A candy-bar type mobile phone with Planar Inverted-F Antenna (PIFA) is used to radiate dual-band frequency of GSM900/1800 in the vicinity of the SAM head phantom. The mobile phone casing is made out of plastic, and only two components are considered: the FR-4 ground plane and PIFA. The specific absorption rate (SAR) averaged over a mass of 10 gram and 1 gram is calculated after obtaining the power loss density and electric field value from simulation in CST Studio Suite 2011. The SAR and return loss results of six hand structures, including the SAM hand phantom are compared. The antenna performance with the inclusion of hand does not decrease as much as 1800 MHz in 900 MHz range, but absorbs energy more in the hands for 1800 MHz than 900 MHz SAR values.

1. INTRODUCTION

Concern of possible health effects due to electromagnetic field exposure [1–7] has come to public knowledge since mobile phones became a necessity of life instead of just a desire to have one. More and more people want to know whether any confirmed effects have been stated yet [8] and how to overcome the matter without stopping the usage [9–13], resulting in on-going research for decades to analyze the rate of electromagnetic wave being absorbed into a specific averaged mass of tissue of a human body [9, 14–33] and even animals [34–36]. The value is obtained by measuring the time rate of RF energy absorption which is given in terms of specific absorption rate (SAR) at various part of body, for example head and hand in the case of mobile phone [20, 22, 23, 25, 26, 28–33]. SAR can be defined as:

$$SAR = \frac{\sigma |E|^2}{\rho} \qquad (1)$$

where $|E|$ is the rms value of the induced electric field (V/m), σ the electrical conductivity of the tissue (S/m), and ρ the density of the tissue (kg/m^3) [14, 27, 37].

Several studies have been done to investigate the maximum value of SAR for various brand of mobile phone [19, 22, 28, 30] to make sure that manufacturers keep their design of mobile phone antenna within safety limits, whether it is a candy-bar-typed phone, a clamshell-type, a mobile phone with a Planar Inverted-F Antenna (PIFA), a dipole antenna [7, 38] or a dipole antenna [19–22]. After the influence of hand emerged in the performance of a mobile phone [12], many researchers have included hand with skin, muscle and bone properties in their simulations. Each hand studied — human's or phantom's — is different in its orientation [25, 26, 38] and its size based on the age [39] and race of the human being studied [6, 31].

In terms of hand grip, Al-Mously and Abousetta [29] investigated the impact of hand-hold positions on both antenna performance and the SAR induced in the user's head. A mobile phone in a hand model close to a Specific Anthropomorphic Mannequin (SAM) head at both cheek- and tilt-positions, according to IEEE-1528 standard (2003), is considered during the simulation. A semi-realistic hand model consisting of three tissues, skin, muscle, and bone, is designed with two different holding positions: grasping the lower part and the upper part of mobile phone. The results show that in the case of the mobile phone in hand close to head at different positions, the antenna's total efficiency reduces at both cheeks and in tilt position, whereas the value of peak averaged SAR at 1 g in head also reduces at both head positions, depending on the hand-hold position. In addition, holding

the mobile phone close to head (grasping upper part) decreases the antenna efficiency dramatically.

In the present work, the maximum SAR values at different user hand positions and properties, specifically on Asian-sized hand will be investigated. It is hypothesized that with the inclusion of a smaller-sized hand in vicinity to the mobile phone, the absorption of RF energy into brain tissue might be increased since it has less absorption in the hand.

2. METHODOLOGY

The designs and simulations will be conducted in CST Studio Suite 2011 [48] which embeds CST Microwave Studio for fast and accurate 3D EM simulation of high frequency problems. Transient Solver is used to solve electric field value, power loss density and S-parameters. Using a T5500 Dell Workstation with Intel Xeon processor, a Fast Perfect Boundary Approximation (FPBA) mesh technology is used to define fine meshes at high dielectric properties area with reduced total simulation time from subgridding scheme. SAR calculation will be performed at $10\,\mathrm{g}$ and $1\,\mathrm{g}$ averaging mass after transient solver stops.

2.1. Mobile Phone

A dual band PIFA with ground plane made of Flame Retardant 4 (FR-4) printed circuit board (PCB) is taken from a clam-shell mobile
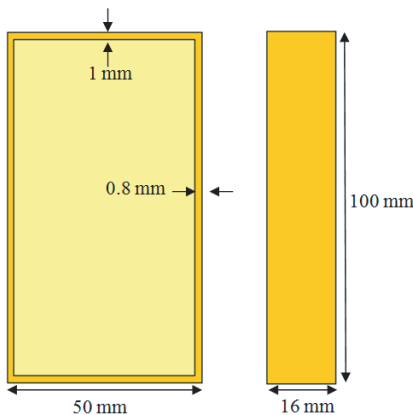

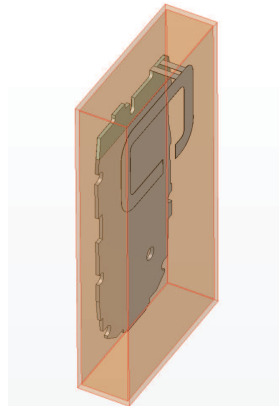**Figure 1.** Dimension for candy-bar mobile phone case.

Figure 2. PIFA and ground plane in plastic casing.

phone in CST Tutorial examples which is then converted into a candy-bar mobile phone by designing a simple plastic box as in Figure 1. Only two components are taken into consideration while others, such as the Liquid Crystal Display (LCD) screen, keypad, circuitry board, Subscriber ID Module (SIM) card and screws are neglected. The fully designed candy-bar mobile phone ready to be used in all simulations is shown in Figure 2.

The phone is first simulated to observe the antenna's efficiency to serve at both GSM frequencies before being simulated together with the presence of head and hand. This is to check whether the casing gives any effects on the reflection coefficient, S_{11} value of the antenna. The phone is then simulated again with Standard Anthropomorphic Model (SAM) head phantom to obtain S_{11} value so that when the hand is included in the later design, any changes in the S-parameters are fully considered by the inclusion. All results of S_{11} for the mobile phone will be shown in the Results and Discussion Section later.

2.2. Hand Model

The initial stage of the research focuses on designing a simple block of hand model based on Malaysian-sized female adult. The quasi-block model is built up using cylinders for the fingers and also bricks for the palm and thumb structure in CST Studio Suite 2011 software. It is also skinned to have cylinders and brick-shaped bones inside to mimic real human hand. The dimension of the hand is shown in Table 1.

Previous research done consists of only solid hand holding a mobile phone close to a human head filled with homogenous glycol-containing tissue-stimulant liquid (TSL) for simulations. The defined liquid is a frequency dependent material according to IEEE/CENELEC/IEC standard which is called Standard Anthropomorphic Model (sometimes

Table 1. Dimension of quasi-block hand model [32].

Hand Dimension	mm
Thumb	50
Index Finger	70
Middle Finger	80
Ring Finger	70
Pinky (Small) Finger	55
Palm	100
Approx. Hand Thickness	20

Table 2. Properties of quasi-block hand model [41–47].

Material	Dielectric Properties	Operating Frequencies	
		900 MHz	1800 MHz
Skin	Epsilon'	41.405	38.785
	E. Conductivity	0.86674	1.1847
Bone	Epsilon'	12.454	11.781
	E. Conductivity	0.14331	0.27522
Solid *	Epsilon'	43.4	37.6
	E. Conductivity	0.88	1.43

*Note: Reference in [40]

Table 3. SAM head TSL [33].

Properties	Operating Frequencies	
	900 MHz	1800 MHz
Epsilon'	41.5	40
Epsilon"	17.98	13.98
Density	1000 kg/m^3	

called Specific Anthropomorphic Mannequin) or SAM. Since the hand is solid without thermal effect and the head filled with TSL, the electromagnetic energy is absorbed only in the head region while the hand is covering the radiating antenna without showing any absorption of radiation. With that, the skin and bone properties for 900 and 1800 MHz are added to the newly designed quasi-block hand model. Both homogenous (solid) and heterogeneous (skin and bone) hand are then compared to see the changes in peak SAR values. The properties are shown in Table 2.

To make good comparisons, both hands must have the same size at an exact position. Although a standard CTIA hand model has already been created with the size of an European hand, a new hand model is used for this study. The solid hand model is made of the same quasi-block hand model, with skin and bone properties merged into one solid property according to the CTIA SAM hand standard. Both hands use the same SAM head with the same TSL defined in Table 3 and also with the same type of mobile phone antenna.

The hand is then imported into the candy-bar mobile phone design to keep the settings of the PIFA from the tutorial example untouched. The hand is moved towards the mobile phone until it is seen holding

the phone on its palm as in Figure 3. With that, the talk-mode position is set up as in Figure 4, and the simulation is run to monitor electric field values and power loss density in order to calculate the maximum rate of absorption for an averaged mass of 10 gram and 1 gram tissues in cubic. The normalized antenna input power is set to 1 Watts for both frequencies. The result will be discussed in the results section later.
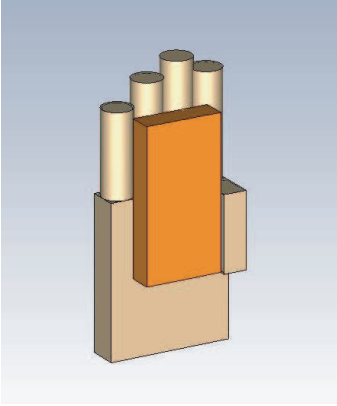

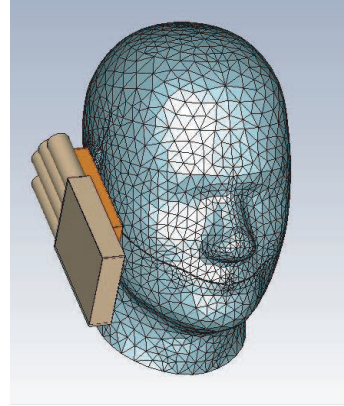
Figure 3. Quasi-block hand model with candy-bar mobile phone [32].

Figure 4. SAR simulation phantom setup [32].
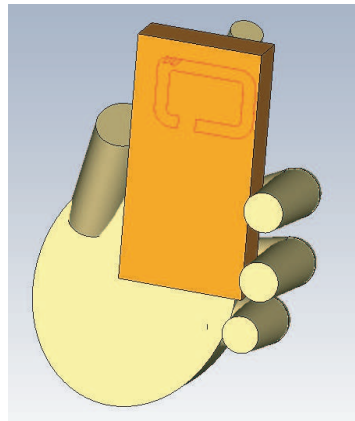
Figure 5. Oval hand phantom grabbing candy-bar mobile phone with PIFA [33].

The second stage is to redesign the quasi-block hand model into a more realistic shape of an Asian-sized hand. The main focus here is to suggest a substitution hand phantom for an Asian who has a smaller-size hand than that of an European. The hand is redesigned to have conical-cylindrical fingers and elliptical palm to resemble a human hand in a normal talk position. The index finger is positioned at the back of the phone where the antenna is radiating, while other fingers are at the side of the phone as shown in Figure 5. The dimensions are almost the same as the earlier version of the quasi-block hand, but a few adjustments are made in order to bend the fingers into a more sensible talk-mode position. The new dimensions are shown in Table 4.

Anatomically, Asians' hands are slightly smaller than Europeans' and might cause the head to absorb part of the energy radiated by the antenna more than the hand does. In order to prove so, the standard CTIA SAM hand is compared with the new oval hand phantom, both solid and having the same dielectric properties, set up together with the same candy-bar mobile phone and SAM head used previously. The setup is shown in Figure 6.

To investigate further on human tissue absorption towards electromagnetic radiation, the oval hand phantom is made in three versions. The first version is the solid hand compared with SAM hand phantom; the second version is similar to the earlier version of brick hand that is skinned to have two dielectric properties of skin and bone shown in Figure 7; the third version is again a bone hand but with the fingers properties defined as tendon and the palm defined as muscle. The properties of both muscle and tendon are referenced in [41–47]. The results of these investigations will be discussed in the result section.

Simulations are done in CST Microwave Studio using T5500

Table 4. Asian-sized hand phantom dimensions [33].

Hand Dimension	mm
Thumb	50
Index Finger	70
Middle Finger	70
Ring Finger	60
Pinky (Small) Finger	50
Palm	100
Approx. Hand Thickness	20

Dell Workstation with Intel Xeon processor in Embedded Computing
Research Cluster, Seriab, Perlis, Malaysia. For discretization, 15 lines
per wavelength with subgridding are chosen in the mesh settings. The
mesh needs to be much finer in the head region due to the high
dielectric permittivity of the brain tissue (TSL). Using hexahedral
Fast Perfect Boundary Approximation (FPBA) mesh technology, the
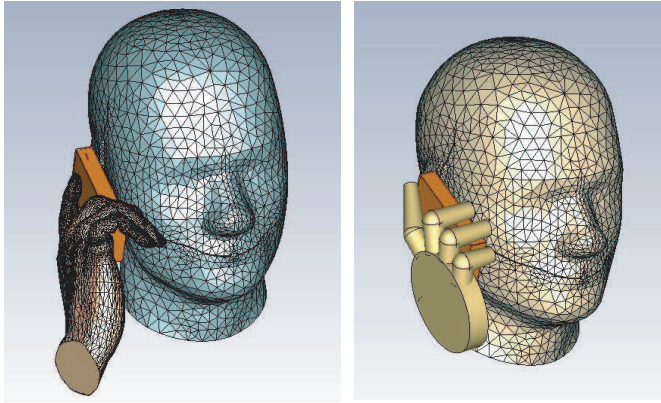transient solver solves electric field and Power Loss Density before
calculating for SAR values.

Figure 6. Simulation setup for both hands [33].
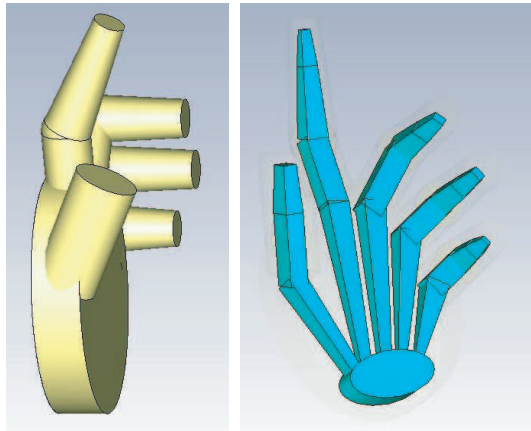
Figure 7. Second version of oval hand phantom (skin and bone).

3. RESULTS AND DISCUSSION

As mentioned previously in Methodology Section, the mobile phone has gone through two simulations to validate the result gained later after
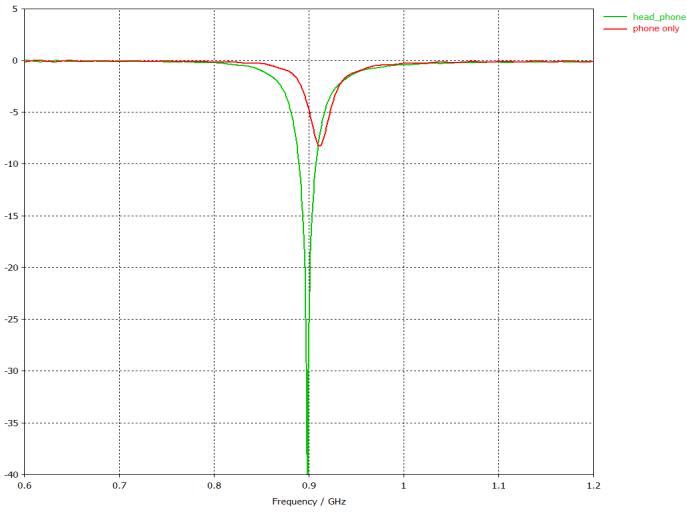
(a)
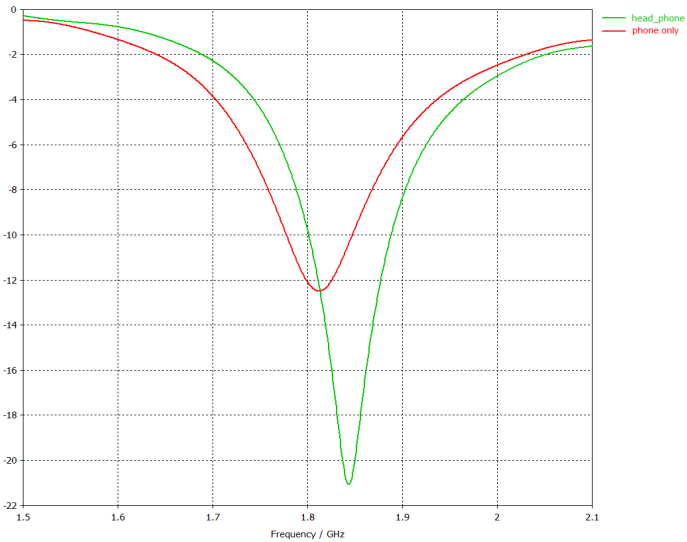
(b)

Figure 8. Return loss for mobile phone between casing and head phantom for (a) 900 MHz and (b) 1800 MHz.

including the proposed hand. The first simulation is between the PIFA and the plastic casing covering it. The return loss for 900 MHz shows a minor shift to the right and drops around -9 dB, while the 1800 MHz also shifts to the right but with less loss at -12 dB (refer to phone only curve). The second simulation (head_phone curve) includes SAM

(a)

(b)
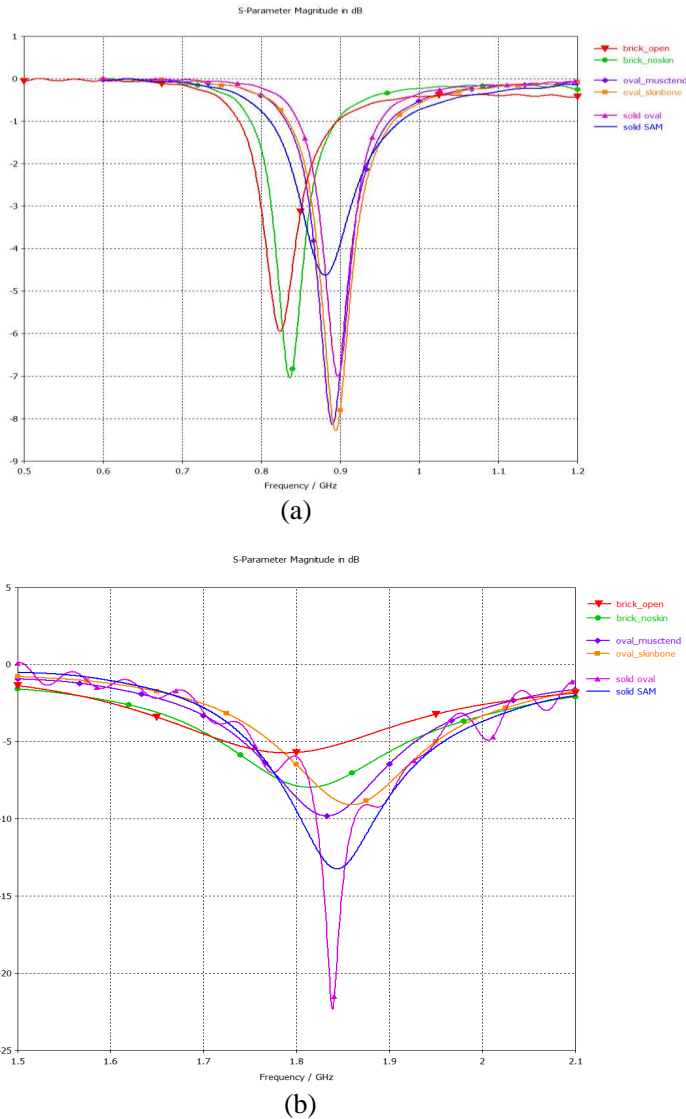
Figure 9. Return loss for all hand structure at (a) 900 MHz and (b) 1800 MHz.

head phantom which shows tremendously good antenna efficiency. It is perfectly tuned for 900 MHz and drops at -40 dB while a shift from 1800 MHz range drops at around -21 dB. The graph for both simulations is shown in Figure 8 for both GSM frequencies.

Figure 9 shows that only the orientation of the oval hand (skinbone and musctend) provides good results for 900 MHz. All the other hands including the solid SAM hand have high return loss and could contribute to low quality calls caused by the high absorption. However, for 1800 MHz, all hand structures cause detuning and some high return loss too.

In terms of SAR results for SAM head phantom in the vicinity of mobile phone and without hand inclusion, both 10 grams and 1 gram averaged mass of head tissue are calculated for both frequencies. Table 5 shows the results of maximum SAR value in XY-plane (ear view) and cutplane-view of XZ-plane to evaluate at both axes the absorption direction into the head. These results also act as a control setup to ensure that any increment or decrement of SAR from the next head-hand setup comes from the inclusion of hand, and with further investigation of the hand positions and tissues involved.

3.1. First Stage

For the first stage simulation involving the quasi-block hand model, two comparisons are made, which are between homogeneous and heterogeneous hands, and between with and without skin hand. Both comparisons take only peak SAR into consideration, whether the peak is in the hand region or in the head region. The purpose at first is to observe how high the SAR could be for that setup.
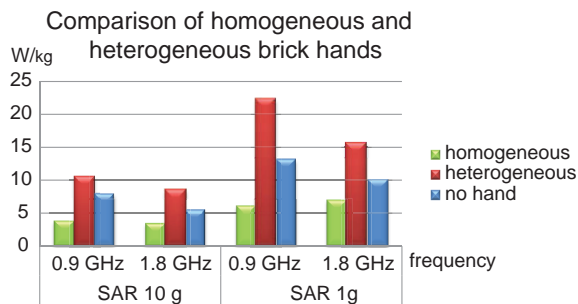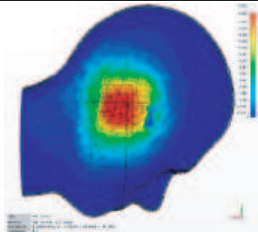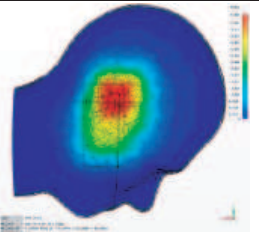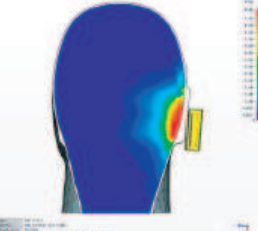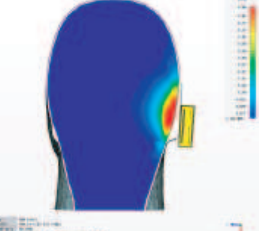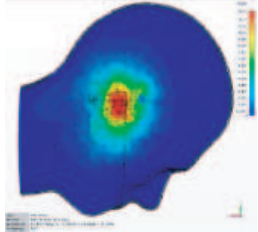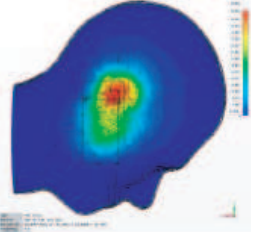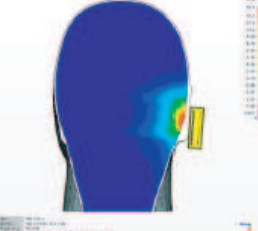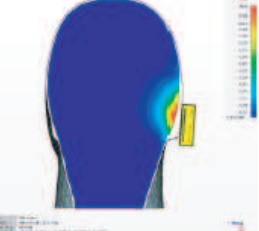

Figure 10. Comparing SAR differences between two types of hands.

3.1.1. Homogenous and Heterogeneous Hand

The electromagnetic field emitted by the candy-bar mobile phone antenna is simulated at two GSM frequencies to see the 3-dimension effect of SAR penetrating the head phantom averaged over a mass of 10 gram and 1 gram cubic. The setup that uses solid hand properties shows that only the head region is absorbing the energy, while the hand

Table 5. Intial SAR values for setup without hands at two axes.

Operating Frequency:	900 MHz	1800 MHz
SAR 10 g — ear view		
SAR 10 g — cutplane view		
Max SAR :	8.03 W/kg	5.48 W/kg
SAR 1 g — ear view		
SAR 1 g — cutplane view		
Max SAR :	13.1 W/kg	10 W/kg

is just there as if not absorbing anything. However, when the hand is defined as absorbing tissues like skin and bone where parameters such as density, heat capacity and thermal conductivity are taken into consideration, there is absorption towards both hand and head region, with the hand absorbing more than the head. The presence of hand as an anatomical material has actually reduced the radiation absorbed by the head.

Results of peak SAR are presented in Figure 10 to make comparisons, and the values are tabulated in Table 6. From the bar chart, it can be seen that the SAR in heterogeneous hand with skin and bone properties is higher than the SAR in solid homogenous hand or without hand. Table 7 shows the location of which part absorbs more energy. Although it shows that the hand absorbed more than the head, the SAR value actually increased compared with that of the homogenous hand. In a way, this is good since the peak SAR value does not come from the head, but still the value in hand region is higher and needs further investigation.

3.1.2. With and without Skin Hand

To determine which tissue absorbes more energy than the other, a simulation on hand with skin (heterogeneous) and hand without skin

Table 6. Maximum SAR values obtained from homogeneous and heterogeneous hands.

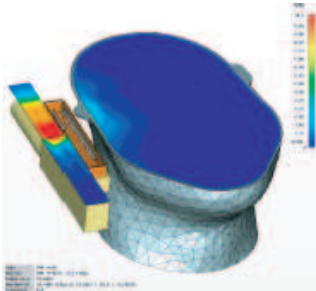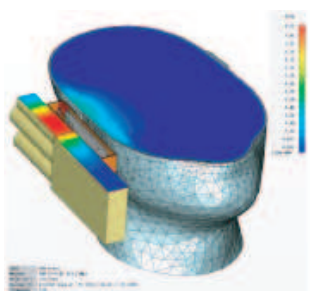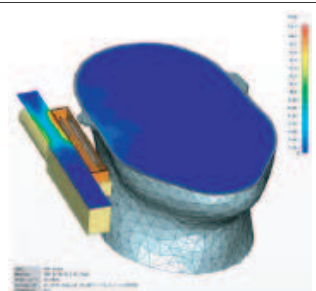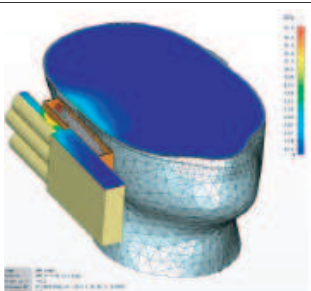| Mass	Homogeneous Hand		Heterogeneous Hand		No Hand	
	900 MHz	1800 MHz	900 MHz	1800 MHz	900 MHz	1800 MHz
10 g	3.81	3.46	10.5	8.52	8.03	5.48
1 g	6.05	6.92	22.3	15.6	13.1	10
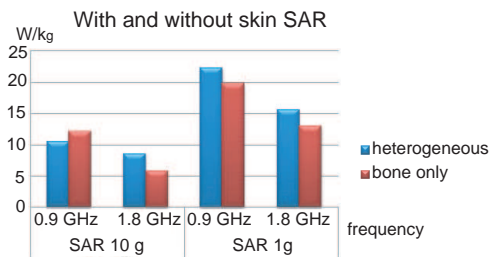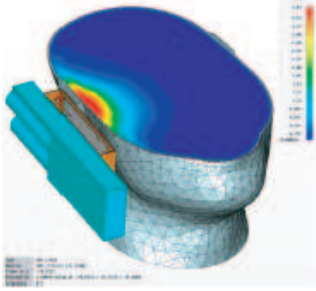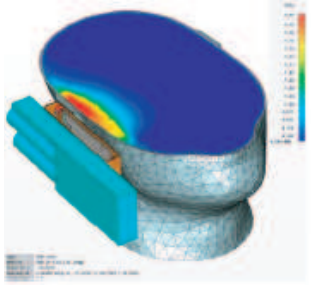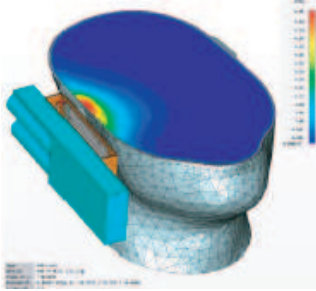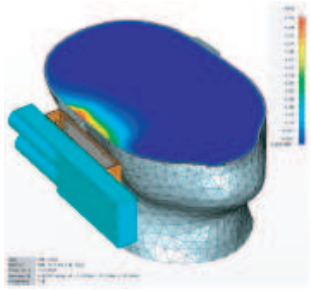
Figure 11. Bar chart for result in Table 4.3.

Table 7. Energy absorbed by head at different hand properties.

		900 MHz	1800 MHz
SAM Hand	SAR 10g		
	SAR 1g		
Quasi-block Hand	SAR 10g		
	SAR 1g		

(bone only) is done. Result from the previous heterogeneous hand is compiled together with the new bone-only hand and tabulated in Table 8. A better comparison is seen in Figure 11.

Table 8. Maximum SAR values obtained from both hands.

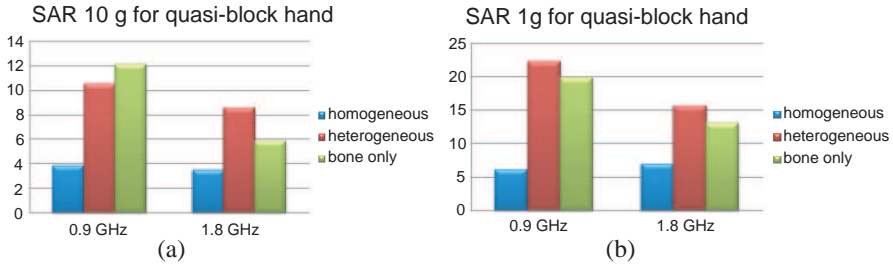| Mass	Heterogeneous		Bone only	
	900 MHz	1800 MHz	900 MHz	1800 MHz
10 g	10.5	8.52	12.1	5.84
1 g	22.3	15.6	19.8	13.0

Figure 12. Comparing (a) SAR and (b) from different structure of hand phantom.

The result obtained from simulated bone-only hand shows that the skin absorbed a small amount of energy, leading the bone part as the major absorber. The bone-only SAR values at an average mass of 1 gram decreases only a bit which might be caused by the actual thickness of skin from the previous hand that is merged all together to be a bone-only hand. The skin thickness is only $\pm 3\%$ larger than the bone and without any air gap in between.

Meanwhile, SAR_{10g} calculation gave uneven results when at 900 MHz, bone-only hand shows increment of absorption, while at 1800 MHz shows otherwise. This phenomena need to be investigated further since the simulation did have some stability issues and reduction of time factor.

In Figure 12, all types of quasi-block hands are then analyzed together in a bar chart to determine which properties absorbs more radiation and contribute to the increment of SAR. Two results are taken from this investigation which is the maximum SAR value at where it peaked, and the maximum SAR value in the head region only. At both frequencies, the structure of skin and bone increases SAR, followed by bone tissue, and this happens at either 10 gram averaging mass or 1 gram. The values are also far from the solid hand that is not filled with any frequency-dependent simulating liquid and that the energy is absorbed fully by the head tissue. Since the important part of human body is the brain, or head tissue, the absorption rate at both 10 gram and 1 gram averaging mass are compared at only 1800 MHz in

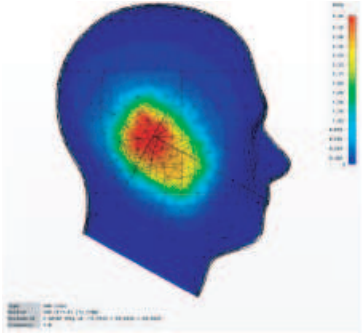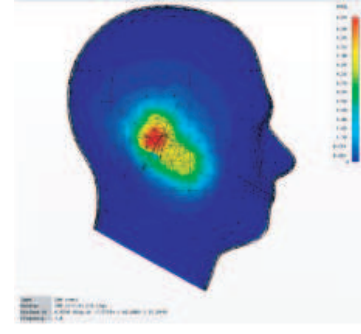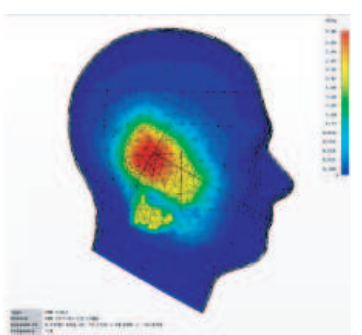**Table 9.** SAR specifically in head region at 1800 MHz.
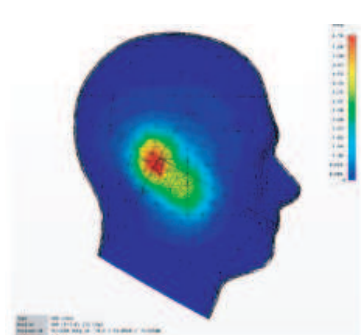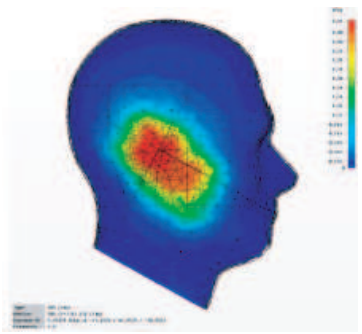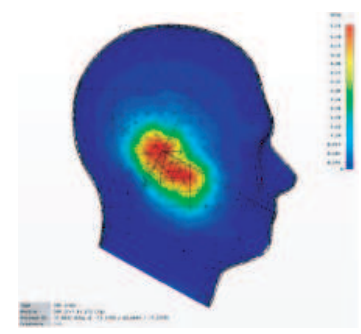
1800 MHz	10 g	1 g
Solid	Max SAR = 3.46	Max SAR = 6.92
Skin + Bone	Max SAR = 3.08	Max SAR = 6.16
Bone only	Max SAR = 3.25	Max SAR = 5.58

Table 9. At this frequency, the wavelength is shorter and the radiation attenuates less deep in human tissues and more at the skin surface.

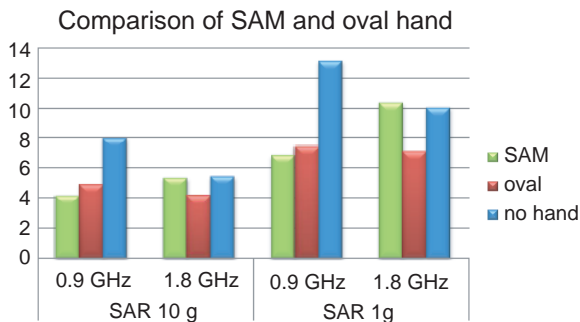In terms of averaged mass of tissue, the calculation of SAR for

Figure 13. Comparing SAR difference between two types of hand.

10 gram is lower than that of the 1 gram tissue most of the time. The American standardized to use 1 gram of cubic-sized tissue to determine the highest value of SAR, and the results should be more precise than a 10 gram tissue SAR which is averaging at a larger size of cube. However, ICNIRP has set the international guidelines and standards for the limit of SAR averaged over a mass of 10 gram.
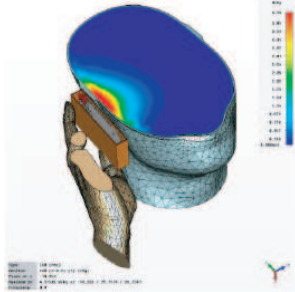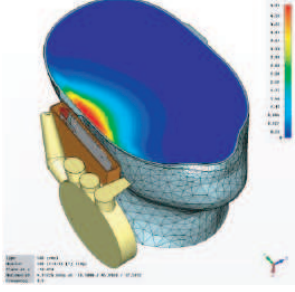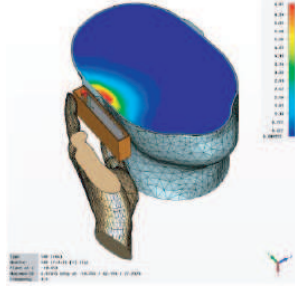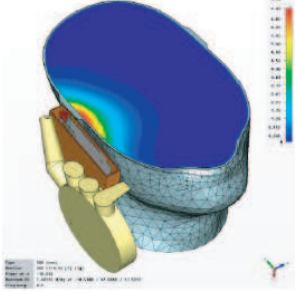
3.2. Second Stage

In the second stage, a more realistic hand is designed, including new tissues such as muscle and tendon in the simulation. For the new oval hand, three sets of hand are designed: a solid hand, skin bone hand, and muscle tendon hand. The muscle tendon hand also includes bone structure inside, but not with the skin on the outside. Instead, the fingers are defined as tendon, and the palm is defined as muscle based on real human hand anatomy.

3.2.1. Solid SAM and Solid Oval

Figure 13 shows the comparison between SAM hand model and oval hand model. The bar chart shows that only 5%–25% difference is obtained compared with both hands. This might be due to the smaller size of Malaysian hand, causing the head to absorb more electromagnetic field than using the SAM hand. There is a decrease of SAR in 1 gram averaged mass of tissue at 1800 MHz from using the oval hand. However, the SAR did increase at 900 MHz for both tissue mass averages. The percentage of SAR between both hands at 900 MHz and 1800 MHz shows a pattern of higher difference at higher frequency but small changes at lower frequency. This is also the same for the no hand result where at lower frequency, the SAR without hand is so

Table 10. Observing the spreading of EM wave into head at 900 MHz.
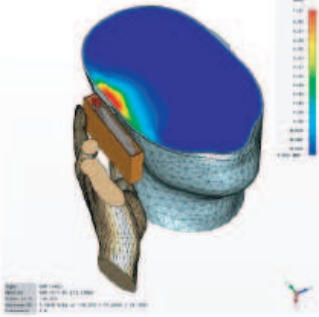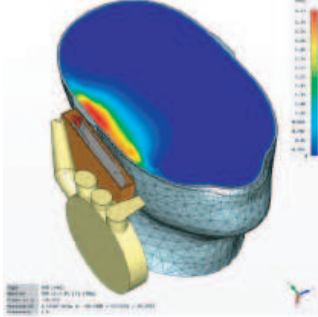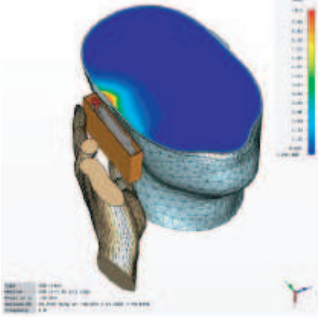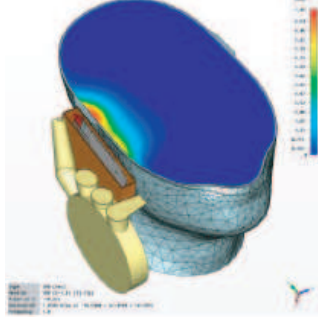
900 MHz	SAM Hand	Oval Hand
10 g	 Max SAR = 4.18	 Max SAR = 4.91
1g	 Max SAR = 6.87	 Max SAR = 7.43

much higher than any of the hand models, but became almost similar
with SAM hand and slightly higher than the oval hand when it reaches
higher frequency.

Another observation is made to see the spreading of the energy
absorbed in the head, shown in Table 10 for lower frequency part,
900 MHz where the absorption is wider in the ear and cheek section
for 10 gram SAR calculation, while for 1 gram SAR the energy absorbs
less in the lower ear section and attenuates faster. With the inclusion
of the suggested oval hand in low frequency, the SAR increases but the
penetration is similar.

In Table 11 for 1800 MHz, only the oval hand at 10 gram SAR
spreads wider in the ear and cheek section, and the others concentrate
more in the ear part and die down quickly. This time, the SAR reduces
but spreads more in the surface for high frequency with the inclusion
of the suggested hand model.

Table 11. Observing the spreading of EM wave into head at 1800 MHz.

1800 MHz	SAM Hand	Oval Hand
10 g	 Max SAR = 5.37	 Max SAR = 4.11
1 g	 Max SAR = 10.3	 Max SAR = 7.06
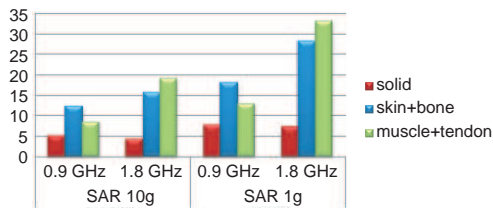
Figure 14. Adding tissue properties to the suggested oval hand model.

3.2.2. Skin Bone Hand and Muscle Tendon Hand

Three hands are compared to analyze which tissue absorbs more radiation than the others, just like the earlier version of quasi-block hand. As seen in Figure 14, the solid hand with no tissue properties has very low SAR at both frequencies compared to the ones structured
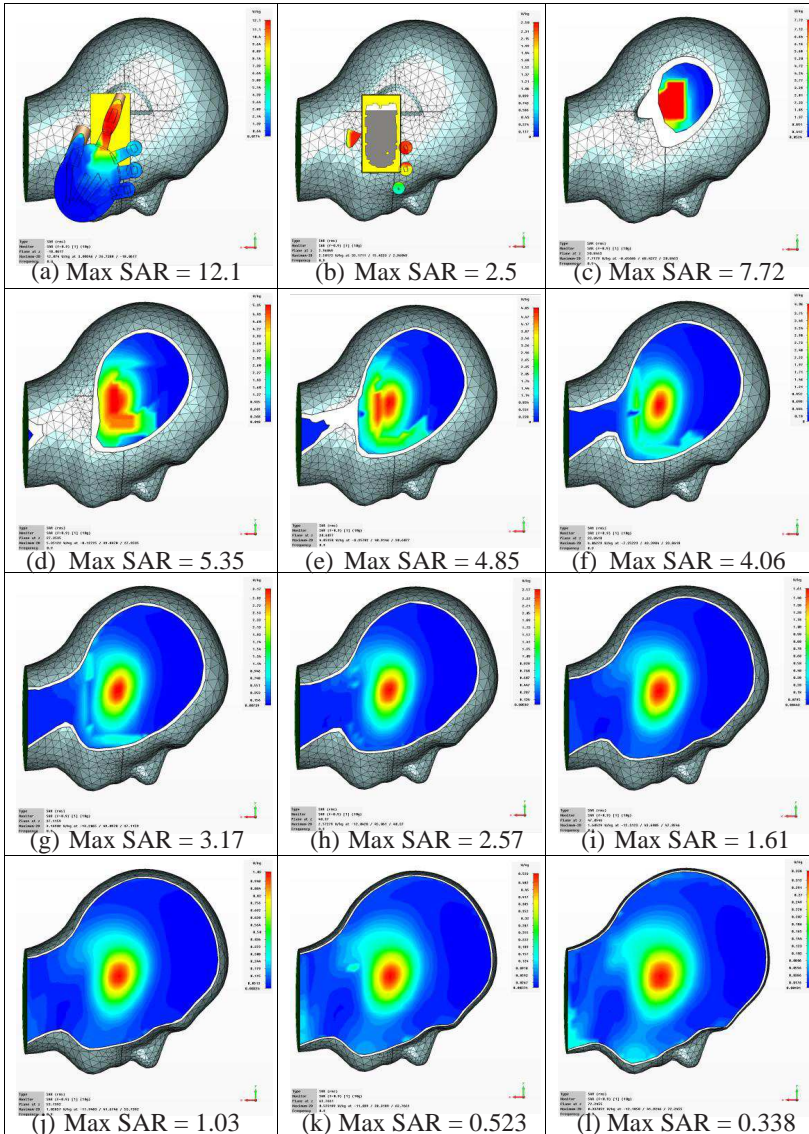
Figure 15. Sliced SAR value from hand to head at 900 MHz for averaged mass of 10 gram.

with hand tissues. As for the hands with tissues properties added, the skin and bone contribute more in the absorption of 900 MHz radiation, but less when the frequency is higher. This phenomenon is vice versa for the muscle and tendon structure which has a higher SAR value at high frequency and then the SAR value decreases compared with the

skin and bone structure SAR value at lower frequency. It can be said
that at low frequency, the skin is a major absorber while at a higher
frequency, the muscle and tendon are the major absorber. The values
are so high that observation of SAR in head region at this particular
orientation is also done.
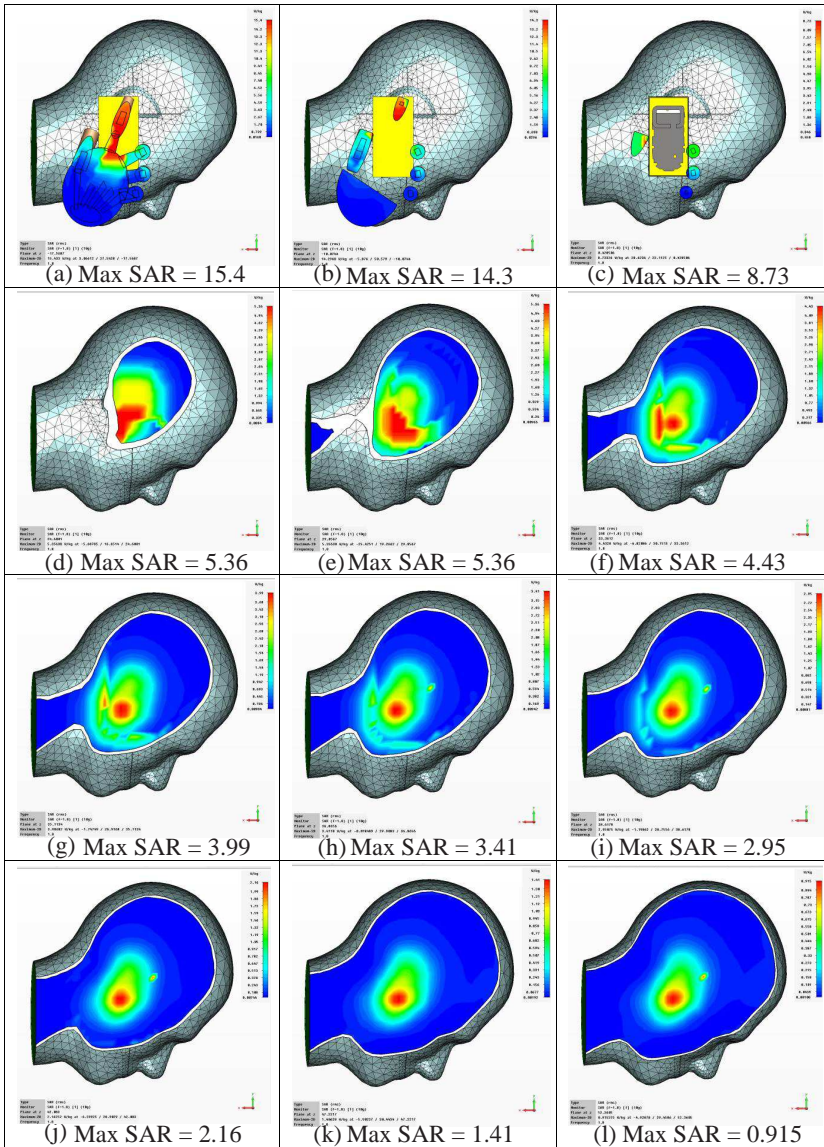
Figure 16. Sliced surface view at 1800 MHz for averaged mass of
10 gram.

Sliced view of each layer penetration in an averaged mass of 10 g is shown in Figure 15 for 900 MHz and Figure 16 for 1800 MHz. By slicing the head phantom, how deep the radiation penetrates can be observed including what is the maximum SAR at each slice. The first figure shows the peak SAR which occurs in the hand region and getting reduced as it goes deeper in head. The maximum SAR in head region is shown on the third figure which is the first open slice of the head. The red position covers the entire ear and heading towards thalamus if a real brain structure is used. As the SAR reduced, it gave no effect towards the tissue and did not heat up any tissue that is marked red.

The highest SAR in the slice view is again in the hand region especially along the index finger close to the PIFA antenna. As the head is sliced, maximum SAR occurs in the cheek part, heading towards the centre of the head as it attenuates further inside. However, the red spots indicating the maximum SAR in deeper slices are more specific with smaller diameters than the ones seen in 900 MHz. The penetration does not die down as quickly as the lower frequency but the

Table 12. Peak SAR of 1 gram averaging for both frequencies.

900 MHz	1800 MHz
Max SAR in hand = 17.9	Max SAR in hand = 28
Max SAR in head = 8.68	Max SAR in head = 18.1
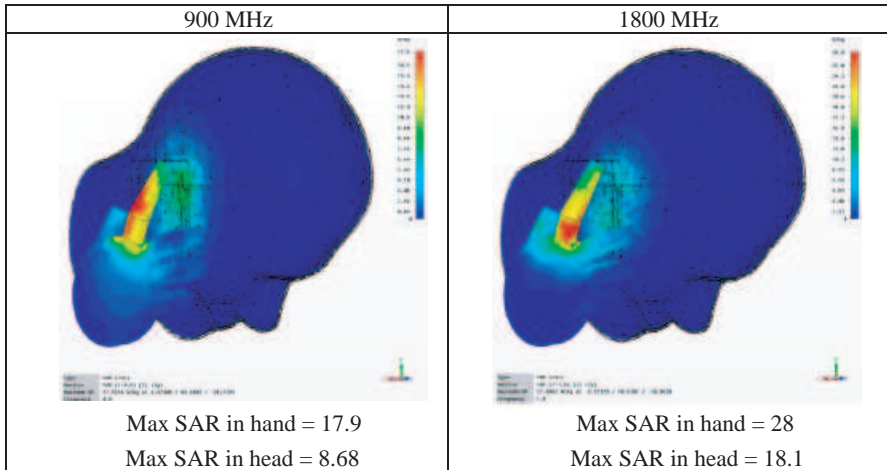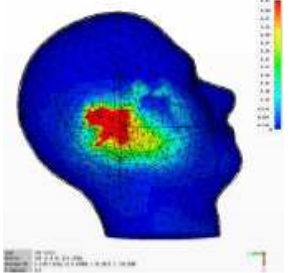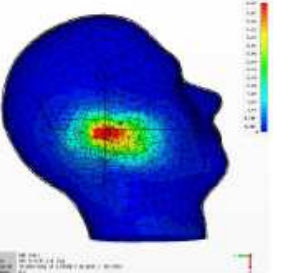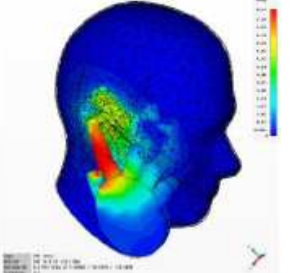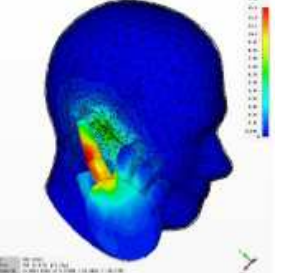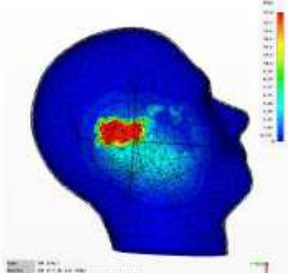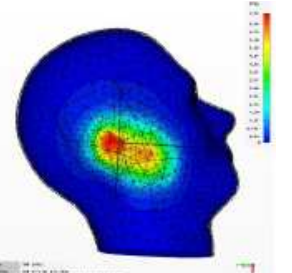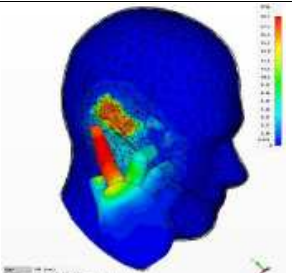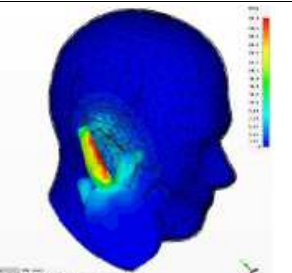
Table 13. Maximum SAR values for muscle tendon hand setup.

Muscle + Tendon + Bone Hand		10 g	1 g
900 MHz	head	5.31	6.47
	hand	8.41	12.9
1800 MHz	head	17	7.25
	hand	19.1	33

Table 14. Peak SAR for head and hand from muscle tendon hand setup.

		10 g	1 g
900 MHz	head		
	hand		
1800 MHz	head		
	hand		

spreading is more focused and longer, which is shown in the fourth and fifth figure where the maximum SAR gives the same value although it has been sliced twice.

As for the 1 gram averaged mass of tissue, both frequencies show the peak SAR in the index finger, but the absorption surface is wider and also lower in the low frequency radiation. The peak SAR obtained in the hands is almost doubled compared with the value in the head, especially the ear part. It can be seen that when frequency is higher, in this case, at 1800 MHz, the maximum SAR is more focused on one small spot rather spreading widely as in 900 MHz. Most of the simulation done from previous work has also shown as stated. Table 12 shows what has been explained.

Table 13 gathers reading from both frequencies and averaging mass and also shows the difference between the peak SARs in head and hand regions. Meanwhile, Table 14 shows the absorption pattern in both regions to observe the spreading. In the muscle tendon hand, the readings are much lower than those in the skin bone hand, which might be caused by the density of the tissues set initially before running the simulation. As the tissues get denser, the radiation becomes harder to penetrate, and this could explain the reason for the much smaller value in the SAR. Although the values look safe, the maximum SAR in head and hand does not change much in the averaging mass of 10 gram. At 900 MHz, the absorption spreads very wide from the upper ear down to the jaw line. The absorption in hand also involves the whole index finger and the upper thumb, both made of tendon tissues surrounding distalis bone. However, in 1 gram averaging mass, the maximum SAR value in hand is twice of that in head and spreads less on the ear and knuckle surface.

The same phenomenon happens for 1800 MHz at 10 gram averaging mass where the value does not change that much in head and hand SARs. The absorption in head region accumulates more in the upper part of ear aligned with the eyes and the whole index finger. The absorption changes to ear and cheek bone parts in the 1 gram averaging mass and also very low compared to the value absorbed by the inner of the index finger which is extremely high, almost five times higher than that of the head maximum value.

4. CONCLUSION

Based on the results and findings from the simulations performed, the main objective of this research has been met which is to investigate various hand positions when holding a mobile phone during talk mode. The results have shown a remarkable assumption that a smaller hand does have significant effect on the rate of energy absorption in head

region compared to the standard hand which is slightly larger than that of the designed hand. It is also obvious that hand inclusion is very important for such an investigation based on the comparison made in this work and must not be left out as in previous work done by others. In fact, various tissues with their own densities have also contributed to a new finding that each tissue has its own absorption capacity and must be included in performing such an investigation to replicate real life conditions. The hand grip also plays a major role in determining the rate of energy absorbed by the head and also the performance of the antenna itself. Although the research focuses on the hand region where the energy absorbed in the hand tissues is always higher throughout the investigation (also seen in [29]). The head region is the most important part that users would not want any unseen energy absorbed. Until now, the effects of SAR are still inconclusive.

REFERENCES

1. Cardis, E., et al., "The INTERPHONE study: Design, epidemiological methods, and description of the study population," *European Journal of Epidemiology*, Vol. 22, No. 9, 647–664, Sep. 2007.

2. Varsier, N., K. Wake, M. Taki, S. Watanabe, E. Cardis, J. Wiart, and N. Yamaguchi, "Categorization of mobile phones for exposure assessment in epidemiological studies on mobile phone use and brain cancer risk," *IEEE Transactions on Microwave Theory and Techniques*, Vol. 56, No. 10, 2377–2384, 2008.

3. Takebayashi, T., et al., "Mobile phone use, exposure to radio frequency electromagnetic field and brain tumor: A case-control study," *British Journal of Cancer*, Vol. 98, 652–659, Feb. 2008.

4. Mohsin, S. A., "Concentration of the specific absorption rate around deep brain stimulation electrodes during MRI," *Progress In Electromagnetics Research*, Vol. 121, 469–484, 2011.

5. Genç, Ö, M. Bayrak, and E. Yaldız, "Analysis of the effects of GSM bands to the electromagnetic pollution in the RF spectrum," *Progress In Electromagnetics Research*, Vol. 101, 17–32, 2010.

6. Yanase, K. and A. Hirata, "Effective resistance of grounded humans for whole-body averaged SAR estimation at resonance frequencies," *Progress In Electromagnetics Research B*, Vol. 35, 15–27, 2011.

7. Khodabakhshi, H. and A. Cheldavi, "Numerical analysis of human head interaction with PIFA antennas in cellular mobile communications," *Progress In Electromagnetics Research B*, Vol. 22, 359–377, 2010.

8. Canbay, C., "The essential environmental cause of multiple sclerosis disease," *Progress In Electromagnetics Research*, Vol. 101, 375–391, 2010.

9. Kusuma, A. H., A.-F. Sheta, I. M. Elshafiey, Z. Siddiqui, M. A. S. Alkanhal, S. Aldosari, S. A. Alshebeili, and S. F. Mahmoud, "A new low SAR antenna structure for wireless handset applications," *Progress In Electromagnetics Research*, Vol. 112, 23–40, 2011.

10. Lin, M.-S., C.-H. Huang, and C.-N. Chiu, "Use of high-impedance screens for enhancing antenna performance with electromagnetic compatibility," *Progress In Electromagnetics Research*, Vol. 116, 137–157, 2011.

11. Chiu, C.-W., C.-H. Chang, and Y.-J. Chi, "Multiband folded loop antenna for smart phones," *Progress In Electromagnetics Research*, Vol. 102, 213–226, 2010.

12. Lin, D.-B., I.-T. Tang, and M.-Z. Hong, "A compact quad-band PIFA by tuning the defected ground structure for mobile phones," *Progress In Electromagnetics Research B*, Vol. 24, 173–189, 2010.

13. Laila, D., R. Sujith, S. M. Nair, C. K. Aanandan, K. Vasudevan, and P. Mohanan, "Mobile antenna with reduced radiation hazards towards human head," *Progress In Electromagnetics Research Letters*, Vol. 17, 39–46, 2010.

14. Yelkenci, T. and S. Paker, "SAR changes in a human head model for plane wave exposure (500–2500 MHz) and a comparison with IEEE 2005 Safety Limits," *Journal of Microwave Power and Electromagnetic Energy*, Vol. 42, No. 2, 64–68, 2008.

15. Omar, A. A., "Complex image solution of SAR inside a human head illuminated by a finite length dipole," *Progress In Electromagnetics Research B*, Vol. 24, 223–239, 2010.

16. Ofli, E. and N. Kuster, "Challenges in complex transmitter development in view of the increasing RF requirements (OTA, SAR, HAC)," *2009 Loughborough Antennas & Propagation Conference*, 72–75, 2009.

17. Gangwar, R. K., S. P. Singh, and D. Kumar, "SAR distribution in a bio-medium in close proximity with rectangular dielectric resonator antenna," *Progress In Electromagnetics Research B*, Vol. 31, 157–173, 2011.

18. Kong, L.-Y., J. Wang, and W.-Y. Yin, "A novel dielectric conformal FDTD method for computing SAR distribution of the human body in a metallic cabin illuminated by an intentional electromagnetic pulse (IEMP)," *Progress In Electromagnetics Research*, Vol. 126, 355–373, 2012.

19. Samsuri, N. A. and J. Flint, "A study on the effect of a metallic ring worn on human fingers using a simple scannable block hand phantom," *2008 Loughborough Antenna* & *Propagation Conference*, 285–288, March 2008.

20. Ofli, E. and N. Kuster, "Challenges in complex transmitter development in view of the increasing RF requirements (OTA, SAR, HAC)," *2009 Loughborough Antennas* & *Propagation Conference,* 72–75, 2009.

21. Zhang, M. and A. Alden, "Calculation of whole-body SAR from a 100 MHz dipole antenna," *Progress In Electromagnetics Research*, Vol. 119, 133–153, 2011.

22. Douglas, M., B. Derat, X. Liao, E. Ofli, and N. Kuster, "Hand phantom models for the assessment of SAR in the head from cellular telephones," *2010 Asia-Pacific Symposium on Electromagnetic Compatibility (APEMC),* 385–388, 2010.

23. Krogerus, J., J. Toivanen, C. Icheln, and P. Vainikainen, "Effect of the human body on total radiated power and the 3-D radiation pattern of mobile handsets," *IEEE Transactions on Instrumentation and Measurement*, Vol. 56, No. 6, 2375–2384, 2007.

24. Gemio, J., J. Parron, and J. Soler, "Human body effects on implantable antennas for ism bands applications: Models comparison and propagation losses study," *Progress In Electromagnetics Research*, Vol. 110, 437–452, 2010.

25. Li, C.-H., E. Ofli, N. Chavannes, and N. Kuster, "Effects of hand phantom on mobile phone antenna performance," *IEEE Transactions on Antennas and Propagation*, Vol. 57, No. 9, 2763–27708, 2009.

26. Li, C.-H., M. Douglas, E. Ofli, B. Derat, S. Gabriel, N. Chavannes, and N. Kuster, "Influence of the hand on the specific absorption rate in the head," *IEEE Transactions on Antennas and Propagation*, Vol. 60, No. 2, 1066–1074, 2012.

27. Moglie, F., V. Mariani Primiani, and A. P. Pastore, "Modeling of the human exposure inside a random plane wave field," *Progress In Electromagnetics Research B*, Vol. 29, 251–267, 2011.

28. Chen, I.-F., C.-M. Peng, and C.-C. Hung, "A faster means to estimate SAR values for mobile phone applications," *IEEE Antennas and Wireless Propagation Letters*, Vol. 8, 994–997, 2009.

29. Al-Mously, S. and M. Abousetta, "A study of the hand-hold impact on the EM interaction of a cellular handset and a human," *International Journal of Electrical and Computer Engineering*, Vol. 3, No. 10, 657–661, 2008.

30. Davis, C. C. and Q. Balzano, "The international intercomparison of SAR measurements on cellular telephones," *IEEE Transactions on Electromagnetic Compatibility*, Vol. 51, No. 2, 210–216, 2009.

31. Martínez-Búrdalo, M., A. Martín, M. Anguiano, and R. Villar, "Comparison of FDTD-calculated specific absorption rate in adults and children when using a mobile phone at 900 and 1800 MHz," *Phys. Med. Biol.*, Vol. 49, 345–354, 2004.

32. Ronald, S. H., M. F. A. Malek, S. I. S. Hassan, M. S. Zulkefli, M. H. Mat, and E. M. Cheng, "A comparative study on the effect of quasi-block hand model specific absorption rate measurement," *2011 Loughborough Antennas and Propagation Conference (LAPC)*, 1–4, Nov. 14–15, 2011.

33. Ronald, S. H., M. F. Abd. Malek, M. H. Mat, and M. S. Zulkefli, "Study of Malaysian-sized hand phantom for GSM900/1800 application," *2012 International Conference on Biomedical Engineering (ICoBE)*, 335–337, Feb. 27–28, 2012.

34. Usman, A. D., W. F. W. Ahmad, M. Z. A. Ab Kadir, M. Mokhtar, and R. Ariffin, "Microwave effects of 0.9 GHz and 1.8 GHz CW frequencies exposed to unrestrained swiss albino mice," *Progress In Electromagnetics B*, Vol. 36, 69–87, 2012.

35. Chaturvedi, C. M., V. P. Singh, P. Singh, P. Basu, M. Singaravel, R. K. Shukla, A. Dhawan, A. K. Pati, R. K. Gangwar, and S. P. Singh, "2.45 GHz (CW) microwave irradiation alters circadian organization, spatial memory, DNA structure in the brain cells and blood cell counts of male mice, mus musculus," *Progress In Electromagnetics Research B*, Vol. 29, 23–42, 2011.

36. Kalantaryan, V. P., R. Martirosyan, L. Nersesyan, A. Aharonyan, I. Danielyan, H. Stepanyan, J. Gharibyan, and N. Khudaverdyan, "Effect on tumoral cells of low intensity electromagnetic waves," *Progress In Electromagnetics Research Letters,* Vol. 20, 97–105, 2011.

37. Attaro, E. A., T. Isernia, and G. Vecchi, "Field synthesis in inhomogeneous media: Joint control of polarization, uniformity and SAR in MRI B_1-field," *Progress in Electromagnetics Research*, Vol. 118, 355–377, 2011.

38. Myllymaki, S., A. Huttunen, V. K. Palukuru, H. Jantunen, M. Berg, and E. T. Salonen, "Capacitive recognition of the user's hand grip position in mobile handsets," *Progress In Electromagnetics Research B*, Vol. 22, 203–220, 2010.

39. Ibrani, M., L. Ahma, E. Hamiti, and J. Haxhibeqiri, "Derivation of electromagnetic properties of child biological tissues at radio frequencies," *Progress In Electromagnetics Research Letters*,

Vol. 25, 87–100, 2011.

40. MCL-T., "Carbon-silicone hand phantoms for phone testing: Material conductivity and permittivity compared to hand tissues," Retrieved June 22, 2011, from SAM Phantom: http://www.sam-phantom.com/handsbackground.php.

41. Dielectric Properties of Body Tissues Website, Italian National Research Council, Institute for Applied Physics, Florence, Italy, http://niremf.ifac.cnr.it/tissprop/.

42. Cole, K. S. and R. H. Cole, "Dispersion and absorption in dielectrics: I. Alternating current characteristics," *Journal of Chemical Physics*, 341–351, April 1941.

43. Gabriel, C. and S. Gabriel, "Compilation of the dielectric properties of body tissues at RF and microwave frequencies," Internet document, URL: http://www.brooks.af.mil/AFRL/HED/ hedr/reports/dielectric/home.html (authorized mirror at http:// niremf.ifac.cnr.it/docs/DIELECTRIC/home.html), Appendix C: Modelling of the data (authorized mirror at http://niremf.ifac.cnr. it/docs/DIELECTR-IC/AppendixC.html).

44. Gabriel, C., "Compilation of the dielectric properties of body tissues at RF and microwave frequencies," Report N.AL/OE-TR-1996-0037, Occupational and environmental health directorate, Radiofrequency Radiation Division, Brooks Air Force Base, Texas, USA, June 1996.

45. Gabriel, C., S. Gabriel, and E. Corthout, "The dielectric properties of biological tissues: I. Literature survey," *Phys. Med. Biol.*, Vol. 41, 2231–2249, 1996.

46. Gabriel, S., R. W. Lau, and C. Gabriel, "The dielectric properties of biological tissues: II. Measurements in the frequency range 10 Hz to 20 GHz," *Phys. Med. Biol.*, Vol. 41, 2251–2269, 1996.

47. Gabriel, S., R. W. Lau, and C. Gabriel, "The dielectric properties of biological tissues: III. Parametric models for the dielectric spectrum of tissues," *Phys. Med. Biol.*, Vol. 41 2271–2293, 1996.

48. CST Microwave Studio in CST Studio Suite 2011 User's Manual, www.cst.com.